Supplementary Materials for

A Conserved Mechanism for Centromeric Nucleosome Recognition by Centromere Protein CENP-C

H. Kato, J. Jiang, B.-R. Zhou, M. Rozendaal, H, Feng, R. Ghirlando, T. S. Xiao, A. F. Straight, Y. Bai*

*To whom correspondence should be addressed. E-mail: yawen@helix.nih.gov

This PDF file includes:

Materials and Methods

Table S1-S5

Fig. S1 -S15

References

Materials and Methods

Protein sample preparation and nucleosome reconstitution

Histones were expressed and purified as described previously (*15*). CENP-C fragments were expressed as GST-fusion proteins and purified as described previously (*5*), followed by an additional reverse-phase HPLC step. Mutations were introduced using QuikChange kit (Stratagene, CA). Uniform ^{15}N and ^{13}C labeling of proteins was obtained by growing cells in M9 medium containing ^{15}N-ammonium chloride and $^{13}C_6$-glucose. The methyl-labeling of histones followed the procedure of Tugarinov et al. (*14*). The nucleosome was reconstituted from recombinant *Drosophila* histones and 167 bp DNA fragment (601 sequence) as described previously (*15*).

NMR spectroscopy

NMR spectra were collected using Bruker 500, 700 and 900 MHz spectrometers. The backbone assignments of CENP-$C_{426-537}$ and the histone H2A/H2B (globular domain) dimer were obtained by analyzing HNCACB, CBCA(CO)NH, HN(CA)CO and HNCO 3D spectra. The CENP-$C_{426-537}$ was in 20 mM sodium phosphate buffer and 1 mM DTT at pH 6.0 and 25^{o}C. The H2A/H2B dimer was in 20 mM sodium phosphate buffer, 0.1 M NaCl and 1 mM DTT at pH 6.0 and 35°C. To monitor the chemical shift changes of the methyl groups in the nucleosome upon binding to CENP-$C_{426-537}$, the methy-TROSY spectra were measured in the absence or presence of 1.5-fold of deuterated CENP-$C_{426-537}$ fragment at 35°C. Leu20 and Val35 in the N-terminal tail of $H3_{1-132}$-LEEGLG were mutated to Ala to reduce signal overlap in the H3-labeled sample. Methyl CSP values were calculated from CSP = $[(\Delta\delta^1H(ppm))^2 + (\Delta\delta^{13}C(ppm) \times 0.17)^2]^{1/2}$ for each methyl group. For binding studies of CENP-$C_{426-537}$ to the $(H3\text{-}LEEGLG/H4)_2$ tetramer, the CENP-$C_{426-537}$ fragment and tetramer were mixed at a molar ratio of 1 (CENP-C) : 2 (tetramer) in 20 mM sodium phosphate, 0.2 M NaCl and 1 mM DTT (pH 6.0) and the HSQC spectrum was collected at 20°C. For the binding of CENP-C motif to the H2A/H2B dimer, the rat CENP-C motif fragment (Pro710-Val742) and the H2A/H2B dimer were mixed at a molar ratio of 1:1. Backbone

amide ^{1}H and ^{15}N CSP values were calculated from CSP = $[(\Delta\delta^{1}H(ppm))^{2} + (\Delta\delta^{15}N(ppm)/5)^{2}]^{1/2}$. All NMR spectra were processed using NMRPipe (*29*) and analyzed with Sparky (http://www.cgl.ucsf.edu/home/sparky/). We note that NOEs among methyl protons in the nucleosome (observed at 45^{o}C) become unobservable at 35^{o}C (*15*). At 45^{o}C, the CENP-C/nucleosome complex is not stable. In addtion, the central region of CENP-C binds to DNA non-specifically. Therefore, transfer-NOE studies with a mixture of nucleosome and excess amount of CENP-C for obtaining more distance constraints were not pursued since non-specific binding of CENP-C to DNA would complicate the interpretation of NOE data. For Leu and Val residues, the averaged chemical shift perturbation or paramagnetic relaxation enhancement value of the methyl groups in the same residue is used.

Spin labeling experiments

The lyophilized powder of CENP-$C_{484-537}$ fragment with a single Cys mutation at a selected position (Phe500, Val509, Val517, Ile523 and Ser535) was dissolved in 20 mM Tris-HCl and 5 mM DTT (pH 8.0) and incubated at room temperature for 30 minutes. DTT was removed by buffer exchange on a G-25 Sephadex column equilibrated with 50 mM sodium phosphate and 0.1 M NaCl (pH7.8). A 10-fold excess of (1-oxyl-2,2,5,5-tetramethyl-3-pyrroline-Δ^{3}-methyl) methanethiosulfonate (MTSL; Toronto Research Chemicals) was added to the peptide solution. The reaction was allowed to proceed overnight at room temperature. The completion of labeling was confirmed by mass spectrometry. The sample was then passed through a G-25 column equilibrated with NMR buffer (20 mM sodium phosphate, pD 6.0) and concentrated using an Amicon Ultra centrifugal unit with a cutoff size of 3 kDa. The spin-labeled fragment was mixed with nucleosomes at a molar ratio of 1 (nucleosome) : 1.5 (CENP-C) in 20 mM sodium phosphate (pD 6.0) (the NMR buffer) and methyl-TROSY spectrum was measured at 35°C. The MTSL spin label was then reduced with a 5-fold excess of ascorbic acid and a second set of methyl-TROSY spectrum was measured.

ITC experiments

The calorimetric titrations of nucleosomes with various CENP-C fragments were performed using a MicroCal VP-ITC titration microcalorimeter at 25°C. For the binding assays using the fragment of the central region of human CENP-C, nucleosome containing $H3_{1-132}$-LEEGLG (5 μM) was titrated with the human CENP-$C_{444-537}$ fragment (100 μM) in a buffer containing 50 mM sodium phosphate, 50 mM NaCl and 1 mM DTT (pH 6.0). For measuring interactions with the CENP-C motif fragment, nucleosome containing $H3_{1-132}$-lEGGLG (2.5 μM) was titrated with the peptide (50 μM) corresponding to the rat CENP-C motif (Pro710-Val742) in 10 mM Tris-HCl, 50 mM NaCl, 1 mM DTT and 1 mM EDTA (pH 7.4). The data was fitted to a model with a single set of identical sites.

$$A = 1 + X_t/(n \times M_t) + K_d/(n \times M_t)$$

$$Q = [(n \times M_t \times \Delta H \times V_o)/2]\{A - [A^2 - 4X_t/(n \times M_t)]^{1/2}\}$$

Here K_d is the equilibrium dissociation constant, V_o is active cell volume, n is the number of binding sites, X_t is the total concentration of the CENP-C fragment, M_t is the total concentration of nucleosome, and Q is the total heat content of the solution contained in V_o.

Cell and extract experiments

The localization of wild type and mutant versions of CENP-C and the central domain of CENP-C were determined by quantitative immunofluorescence of transiently transfected GFP fusions to each protein. HeLa cells were seeded at a 100,000 cells per well in a 12 well dish one day prior to transfection. Cells were then transfected with 1 μg of the indicated pEGFP-C1-CENP-C constructs with FuGene 6 transfection reagent (Promega), using a ratio of DNA:FuGene of 1:3. Twenty four hours after transfection, cells were replated onto poly-L-lysine coated coverslips for two hours and then fixed for 5 minutes in 2% formaldehyde in PBS. Fixed cells were blocked in antibody dilution buffer (AbDil = TBS (20 mM Tris pH7.4, 150 mM NaCl) containing, 0.1% v/v Triton X-100, 0.1% sodium azide and 2% bovine serum albumin) and then stained for 45 minutes with Alexa488

conjugated llama anti-GFP (1 μg/ml) and Alexa568 conjugated rabbit anti-hsCENP-T (1 μg/ml) diluted in AbDil. Cells were then stained for 5 minutes with 10 μg/ml Hoescht 33258 in AbDil followed by fixation and mounting in 90% Glycerol, 20 mM Tris-HCl pH 8.8, 0.5% p-phenylenediamine. Fluorescence imaging was performed on an Olympus IX70 using a 60 X 1.4 Plan Apo objective lens (Olympus), CoolSnap-HQ CCD camera (Photometrics Inc) and images were captured with DeltaVision softWoRx software. All image processing was done with custom software (http://straightlab.stanford.edu/software). Chromatin array experiments using *Xenopus* egg extracts were performed as previously described (*6*).

Crystallization, Data Collection and Structure Determination

A rat CENP-C motif peptide PNVRRSNRIRLKPLEYWRGERIDYQ corresponding to residues 710-734 was synthesized by United Biosystems, Inc (Herndon, VA). The peptide was mixed with the nucleosome containing $H3_{1-132}$-IEGGLG and 147 bp DNA (601 sequence) (NCP147) at a 3:1 molar ratio. The complex was purified using Superose 6 size exclusion column (GE healthcare) and concentrated to 13-20 mg/ml for crystallization. Crystals of the complex were grown at 18°C using hanging drop vapor diffusion method in 3-7 days. The crystallization drops were composed of an equal volume mix of the complex at ~15 mg/ml and a solution of 10% MPD, 40mM sodium cacodylate pH 7.5, 24mM spermine tetra-HCL, 80mM sodium chloride and 20mM magnesium chloride. The reservoir solution was 35% MPD. Crystals were harvested with the reservoir solution as cryoprotectant before cryo-cooling by plunging into liquid nitrogen. X-ray diffraction data were collected at GM/CA-CAT (beamline 23ID-D) at the Advanced Photon Source (APS). The diffraction data were processed with programs HKL2000 (*30*) and XDS (*31*). The structure was determined by molecular replacement method using the *Drosophila* nucleosome structure 2PYO (*32*) as the search model with program Phaser (*33*) in the PHENIX suite (*34*). Two copies of nucleosomes were found in the asymmetry unit related by a 2-fold rotation symmetry and tightly packed face-to-face. The calculated electron density map clearly showed

the IEGGLG tail. Following rigid-body and restrained refinement of NCP147 structures with PHENIX, two traces of strong electron density were clearly visible between the two copies of NCP147. The 22 residues of the CENP-C Motif peptide VRRSNRIRLKPLEYWRGERIDY (712-733) were then modeled in the electron density. Further refinement was carried out using the DEN (*35*) method with CNS (*36*) and the 2PYO structure as a reference model. The structure was refined to 3.5 Å resolution with an R_{work} of 23.5% and R_{free} of 28.7% and validated by the Molprobity server (*37*). Note that we also tried to use human CENP-C motif and CENP-A nucleosome for crystallization studies but failed to obtain high quality crystals. The binding constant of the rat CENP-C motif is 14 times higher than that of human CENP-C motif. In addition, the resolution of CENP-A nucleosome is lower than that of the canonical nucleosome. These differences may have led to the successful cryatllization of the rat CENP-C motif in complex with the chimeric nucleosome.

Docking calculation

Guided by the results of the CSP, PRE, and mutation-ITC analyses, we docked the nucleosome binding domain CENP-$C_{519-535}$ to the histones containing H2A/H2B/$H3_{1-132}$-LEEGLG/H4 on one side of the nucleosome structure (pdb ID: 2PYO) using HADDOCK version 2.1 (*38*), installed on the National Institutes of Health Biowulf server. LEEGLG was linked to $H3_{1-132}$ manually using PyMol. (The PyMOL Molecular Graphics System, Version 1.4.1, Schrödinger, LLC.) Histone residues were considered active if they are exposed in the nucleosome structure and show large chemical shift changes or PRE effects on their neighbor residues. All residues in CENP-$C_{519-535}$ were considered active. The initial conformation of CENP-$C_{519-535}$ was built using PyMol. The region of $_{530}$WWVV$_{533}$ in CENP-$C_{519-535}$ was placed close to the LEEGLG tail while the N-terminal region including Arg522 and Arg525 was placed near the acidic patch region. There is no direct contact between CENP-$C_{519-535}$ and the nucleosome. A total of 1,000 structures were generated during the rigid-body energy minimization step (it0), and were subsequently subjected to simulated annealing (it1) during which

the backbone and side chains of the CENP-$C_{519-535}$ and the LEEGLG tail of $H3_{1-132}$-LEEGLG were allowed to move freely. The resulting structures were sorted according to intermolecular energy (sum of the van der Waals, electrostatic, and AIRs energy), and the 200 structures with the lowest energies were selected and analyzed. A structure with close contacts between WWVV of CENP-C and the two Leu residues in LEEGLG and between Arg522 and Arg525 of CENP-C and the acidic patch of H2A/H2B were chosen as the initial structural model. This structure was further relaxed using simulated annealing (it1) during which only side chains of the residues were allowed to move. A structure with the best contacts between residues $_{530}$WWVV$_{533}$ of CENP-C and the two Leu residues in the LEEGLG tail of $H3_{1-132}$-LEEGLG, between residue Arg525 of CENP-C and the residues Asp89 and Glu90 of H2A, and between Arg522 of CENP-C and Glu60 and Glu63 of H2A was chosen as the final structural model. All molecular structures in the paper were drawn using PyMol (http://www.pymol.org).

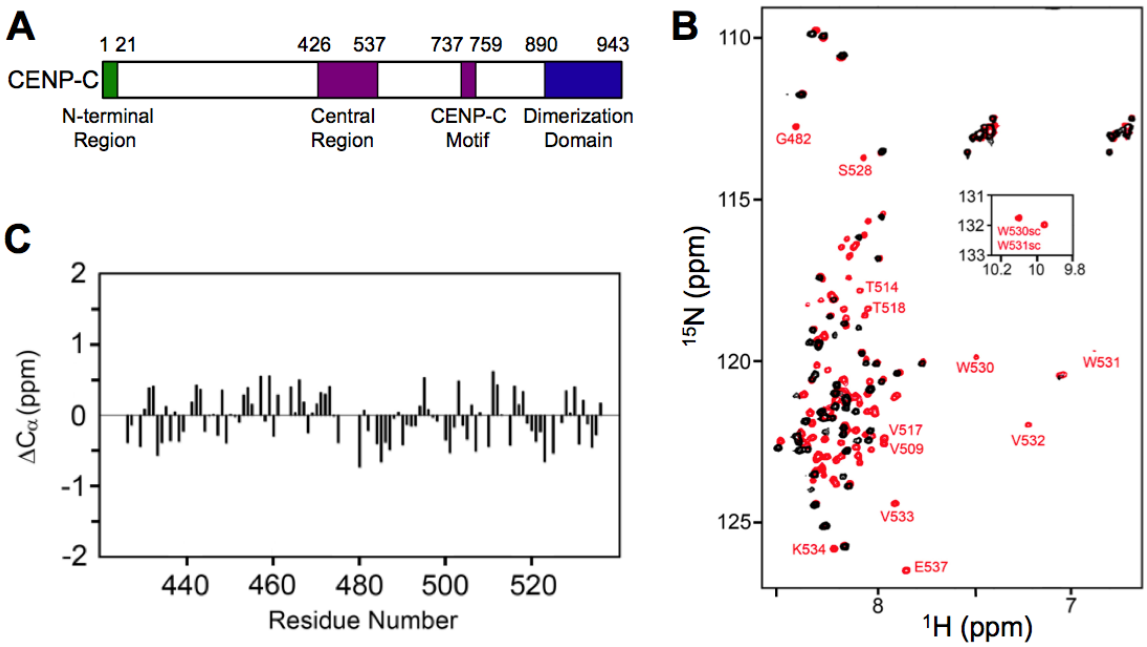

Figure S1. The central region of CENP-C (residues 426-537) is intrinsically disordered and binds to the acidic patch and C-terminal region of $H3_{1-132}$-LEEGLG of the chimeric nucleosome using its C-terminal region (residues 482-537). (**A**) Schematic presentation of functional regions of CENP-C. (**B**) Overlay of the ^{1}H-^{15}N HSQC spectra of CENP-$C_{426-537}$ in free form (red) and bound to the nucleosome containing $H3_{1-132}$-LEEGLG (black). Assignment for some of the residues in CENP-$C_{426-537}$ is shown. W530sc and W531sc represent the side chains of Trp530 and Trp531 respectively (insert). (**C**) Deviation of Cα chemical shifts of CENP-$C_{426-537}$ from the corresponding random coil values.

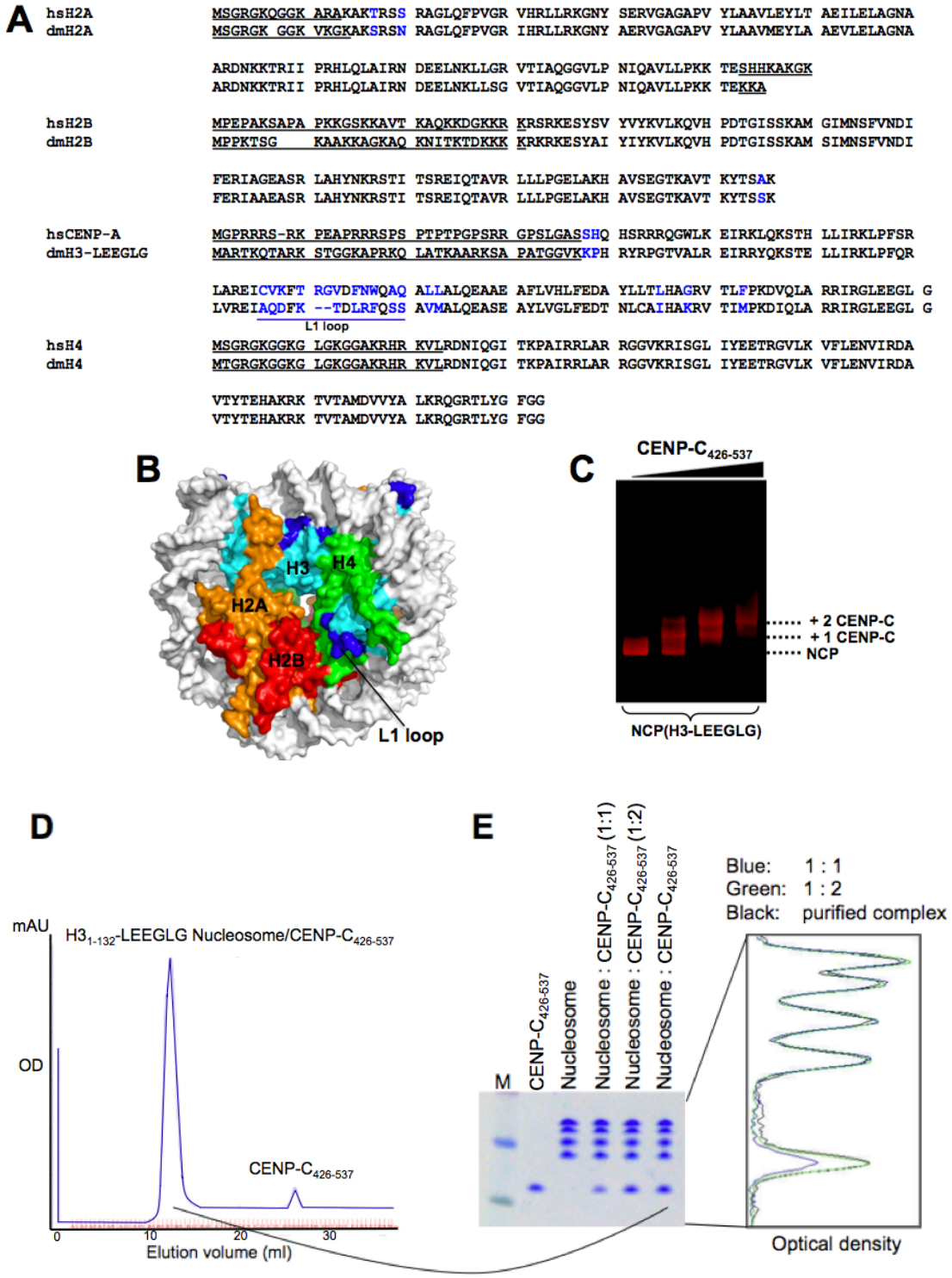

Figure S2. The central region of human CENP-C (CENP-$C_{426\text{-}537}$) binds to the *Drosophila* nucleosome containing $H3_{1\text{-}132}$-LEEGLG. (**A**) Comparison of amino acid sequences of *Drosophila* and human histones. The residues that are not

conserved on the surface of the CENP-A nucleosome structure are colored in blue. (**B**) Diagram showing the conserved surface in *Drosophila* nucleosome containing $H3_{1-132}$-LEEGLG and human CENP-A-nucleosome. The blue regions are not conserved. However, the L1 loop of CENP-A is required for binding of CENP-N (*13*); CENP-N and CENP-C can bind to the CENP-A nucleosome simultaneously (*5*). Thus, the L1 loop of CENP-A/H3 are not involved in the binding of CENP-C. (**C**) Gel shift assay for the binding of CENP-$C_{426-537}$ and the drosophila nucleosome containing $H3_{1-132}$-LEEGLG. Two CENP-$C_{426-537}$ molecules can bind to one $H3_{1-132}$-LEEGLG-nucleosome. (**D**) Separation of the $H3_{1-132}$-LEEGLG nucleosome/CENP-$C_{426-537}$ complex in excess of CENP-$C_{426-537}$ by gel filtration. Note that the gel filtration profile has been overlaid with the lines drawn manually to make it more legible. (**E**) SDS gel of the $H3_{1-132}$-LEEGLG nucleosome/CENP-$C_{426-537}$ complex purified from gel filtration experiment and the mixture of the $H3_{1-132}$-LEEGLG nucleosome with CENP-$C_{426-537}$ in predetermined ratios: 1:1 and 1:2. Overlay of the scanned profiles of the SDS gel of the histones indicates that 1 nucleosome binds to 2 CENP-$C_{426-537}$.

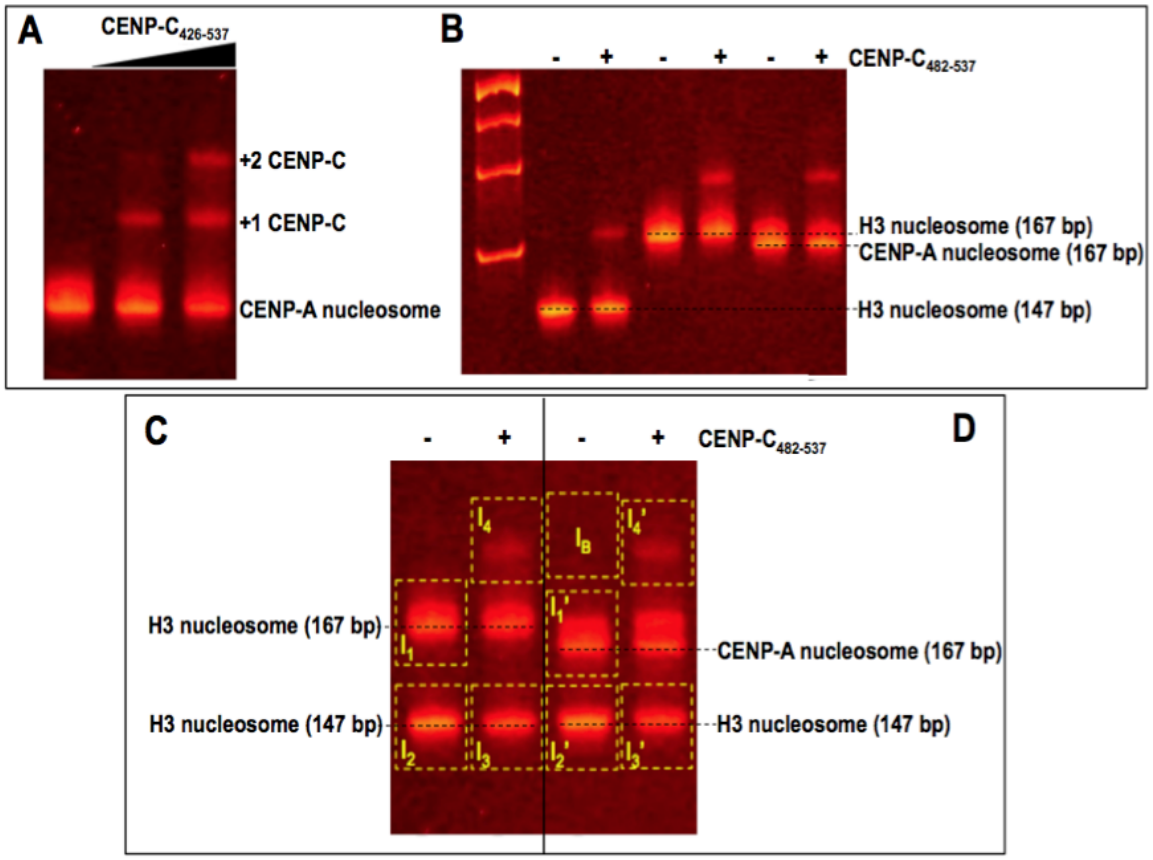

Figure S3. Competition experiments show that the central region of CENP-C binds to the CENP-A and $H3_{1\text{-}132}$-LEEGLG nucleosomes with similar affinity (K_d(CENP-A)/K_d($H3_{1\text{-}132}$-LEEGLG) ≈ 1.3). (Also see **Table S3**, replacement of the corresponding region of $H3_{1\text{-}132}$-LEEGLG by the L1 loop and α2 helix of CENP-A, the CENP-A targeting domain (CATD), which involves 22 mutations, also did not change the binding affinity). This small difference is close to the estimated uncertainty of our experiment.

(**A**) Gel shifts of CENP-A nucleosome by CENP-$C_{426\text{-}537}$, showing that CENP-C binds to the CENP-A nucleosome in two steps similar to the $H3_{1\text{-}132}$-LEEGLG nucleosome.

(**B**) Gel shift results of CENP-A and $H3_{1\text{-}132}$-LEEGLG nucleosomes by small amount of CENP-C, showing different shifts of nucleosomes with 147 and 167 bp DNA.

(**C**) Competition for binding of CENP-C by $H3_{1\text{-}132}$-LEEGLG nucleosome with 147 and 167 bp DNA. In this experiment, the $H3_{1\text{-}132}$-LEEGLG nucleosomes with 147

bp DNA and 167 bp DNA are mixed together and added to two tubes each with 9 μl (~0.1 μM). One of the above two tubes is added with 1 μl CENP-C solution (~0.05 μM) and the other with 1 μl buffer.

(**D**) Competition for binding of CENP-C by $H3_{1-132}$-LEEGLG nucleosome with 147 bp DNA and CENP-A nucleosome with 167 bp DNA. Similar to (**C**), with the exception that the $H3_{1-132}$-LEEGLG (147 bp DNA) and CENP-A (167 bp) nucleosomes are mixed together.

In (**C**) and (**D**), the DNA was stained with ethidium bromide, visualized with UV light, and recorded with a digital camera. The band intensities in the dashed frames were measured using Doc-IT image analysis software (UVP, LLC; California) and subtracted by I_B(baseline): I_1($H3_{1-132}$-LEEGLG, 167), I_2($H3_{1-132}$-LEEGLG, 147), I_3($H3_{1-132}$-LEEGLG, 147), I_4($H3_{1-132}$-LEEGLG, 167, CENP-C), I_1'(CENP-A, 167), I_2'($H3_{1-132}$-LEEGLG, 147), I_3'($H3_{1-132}$-LEEGLG, 147), I_4'(CENP-A, 167, CENP-C).

Combination of (**C**) and (**D**) allows calculation of the ratio of K_d of CENP-C binding to CENP-A nucleosome over that to $H3_{1-132}$-LEEGLG nucleosome with 167 bp DNA using following equations:

For Nuc-CENP-C ⇔ Nuc + CENP-C;

$K_d = [Nuc][CENP\text{-}C]/[Nuc\text{-}CENP\text{-}C]$

K_d(CENP-A, 167)/K_d($H3_{1-132}$-LEEGLG, 167)

$= \{K_d(CENP\text{-}A,167)/K_d(H3_{1-132}\text{-}LEEGLG,147)\}$

$/\{K_d(H3_{1-132}\text{-}LEEGLG,167)/K_d(H3_{1-132}\text{-}LEEGLG,147)\}$

$= \{(I_1'-I_4')(I_2'-I_3')/(I_4'I_3')\} / \{(I_1-I_4)(I_2-I_3)/I_4I_3\}$

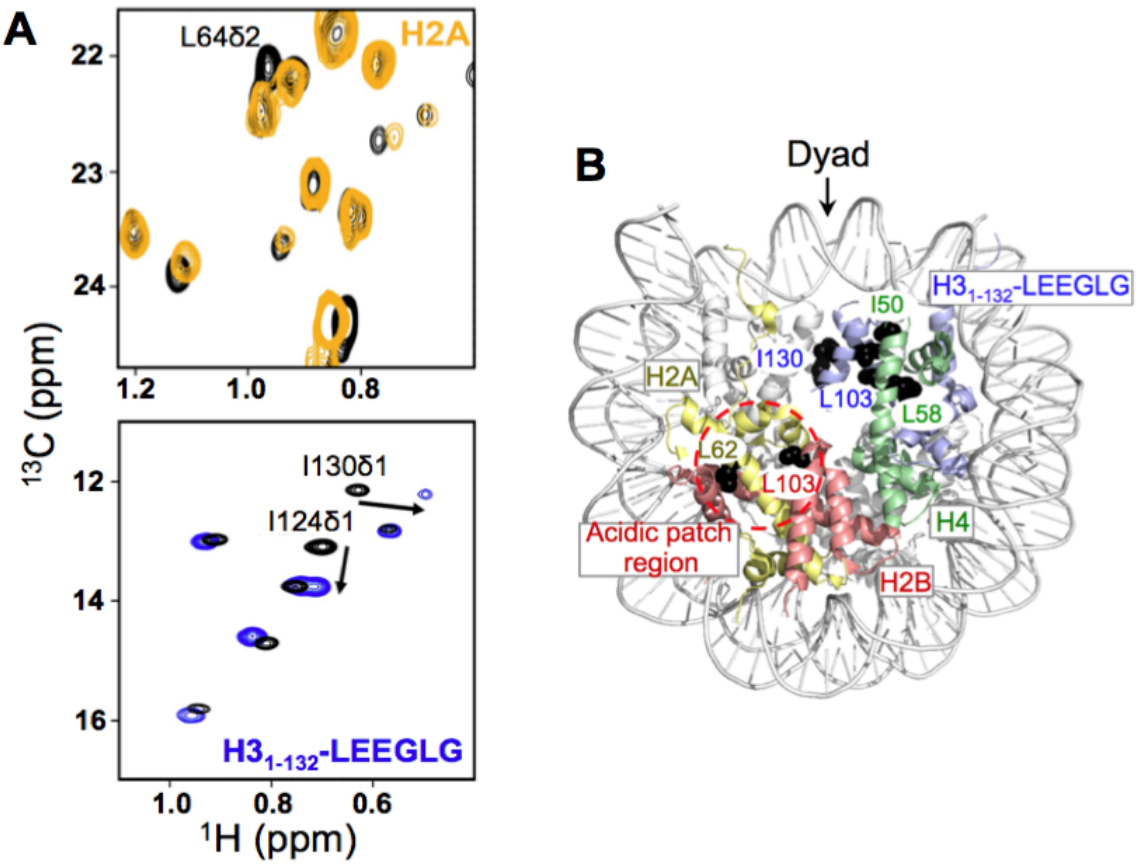

Figure S4. Identification of binding sites of the CENP-C central region on the $H3_{1-132}$-LEEGLG nucleosome by chemical shift perturbation. (**A**) Representative regions of ^{1}H-^{13}C methyl TROSY spectra of H2A and $H3_{1-132}$-LEEGLG in the nucleosome without (black) and with (orange and blue) CENP-$C_{426-537}$. The concentrations of the nucleosomes in these NMR studies were ~100 μM. (**B**) Nucleosome structure showing residue side chains (black balls) whose methyl groups display large chemical shift changes upon CENP-$C_{426-537}$ binding. They are located in the acidic patch (rich in acidic residues) of H2A/H2B, and in the region of H3/H4 surrounding the CENP-A C-terminal tail. We note that it is not feasible to study the CENP-A nucleosome by methyl-based NMR because the expression of CENP-A needs to be done in D_2O and minimum medium, leading to very low yield of proteins. In addition, an NMR sample requires ~300 μl solution with ~100 μM nucleosome.

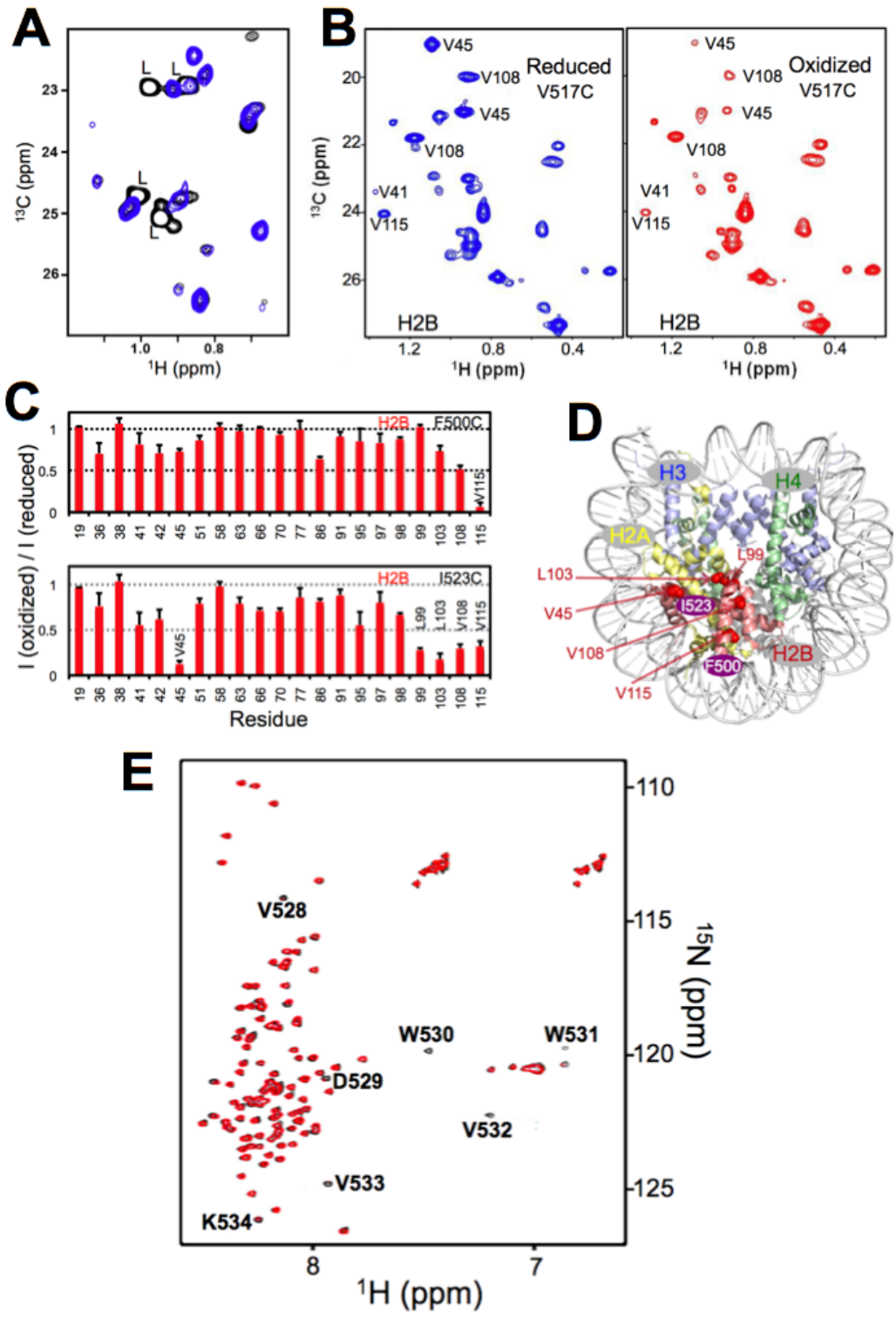

Figure S5. Mapping the binding sites of the central region of CENP-C on the nucleosome containing $H3_{1-132}$-LEEGLG by NMR. (**A**) Overlay of methyl-TROSY spectra of $H3_{1-132}$-LEEGLG in the nucleosome without (black) and with (blue)

CENP-$C_{426-537,}$ showing that methyl groups of the two Leu residues in the C-terminal tails are disordered (strong peaks) but become ordered (disappearance of the strong peaks) upon binding of CENP-$C_{426-537}$. These results indicate that the Leu residues in the tail of $H3_{1-132}$-LEEGLG fold into the nucleosome core upon binding of CENP-$C_{426-537,}$ as is the region 482-537 of CENP-$C_{426-537}$ (fig. S1), representing a disorder-to-order conformational transition. (**B**) Illustration of the effect of spin labeling on methyl signals in the nucleosome. ^{1}H-^{13}C TROSY spectra of histone H2B in the nucleosome that is in complex with reduced (diamagnetic, blue) and oxidized (paramagnetic, red) spin-labels at position Val517 of CENP-C. (**C**) Bar graphs showing the effects of the spin labeling of CENP-C residues Phe500 and Ile523 on the methyl groups of H2B in the nucleosome. (**D**) Structural mapping of the methyl groups that are strongly affected (with decrease of intensities by 50% or more) by the spin labeling of Phe500 and Ile523. (**E**) The peak intensities of the residues in the $_{528}$SDWWVVK$_{534}$ region of CENP-$C_{426-537}$ decreased when mixed with the $(H3_{1-132}$-LEEGLG/$H4)_2$ tetramer. The spectra are for CENP-C with (red) and without (black) the histones, respectively. These results indicate that the $_{528}$SDWWVVK$_{534}$ region of CENP-$C_{426-537}$ binds specifically but weakly to the C-terminal tail of $H3_{1-132}$-LEEGLG in the $(H3_{1-132}$-LEEGLG/$H4)_2$ tetramer.

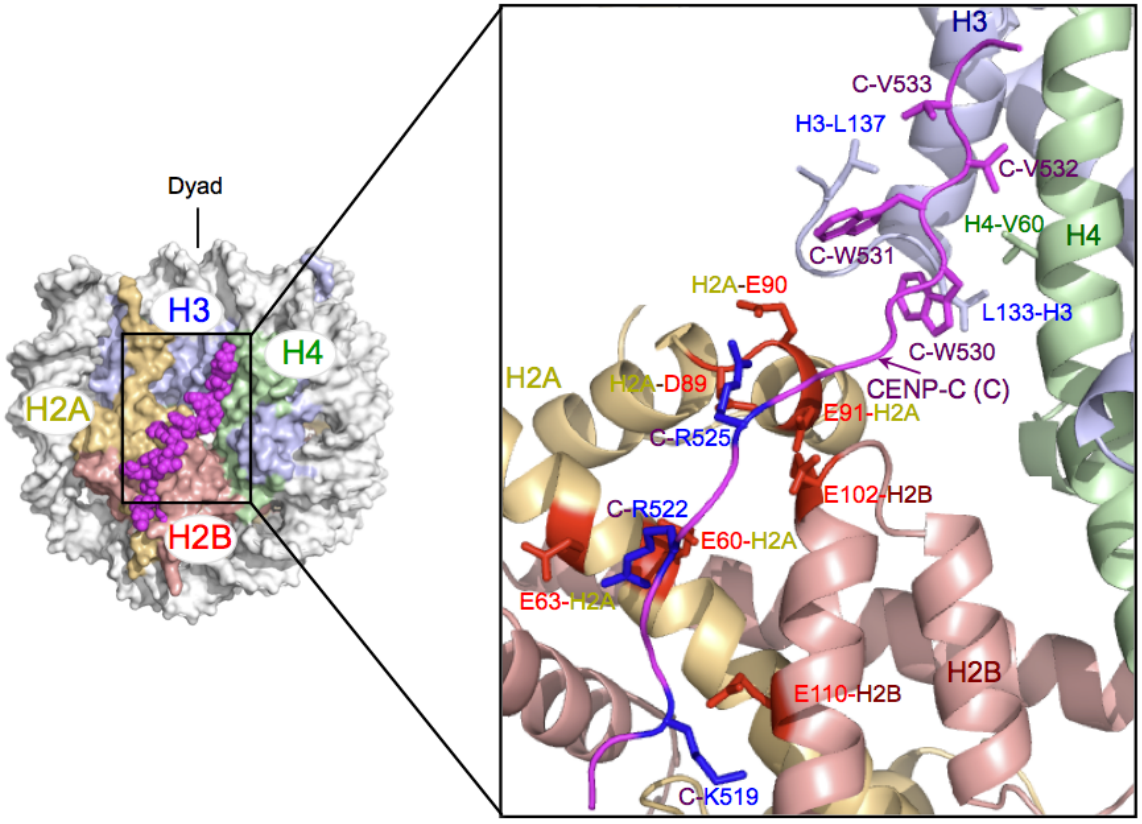

Fig. S6. Illustration of the interactions between CENP-$C_{519\text{-}535}$ and the histones in a structural model. Histones are shown in ribbon with H2A in light orange, H2B in light red, H3 in light blue and H4 in light green. The backbone of CENP-$C_{519\text{-}535}$ is in magenta. Hydrophobic and positively charged residues in CENP-C are presented with magenta and blue sticks, respectively. The acidic side chains of histones are shown in red sticks. The CENP-C residues 482-508, which include many positively charged residues ($_{482}$GSKKSSTRKDKEESKKKRFSSESKNK L_{508}), likely bind to DNA near the C-terminal region of H2B, about 30 bp away from the entry/exit point of the nucleosome.

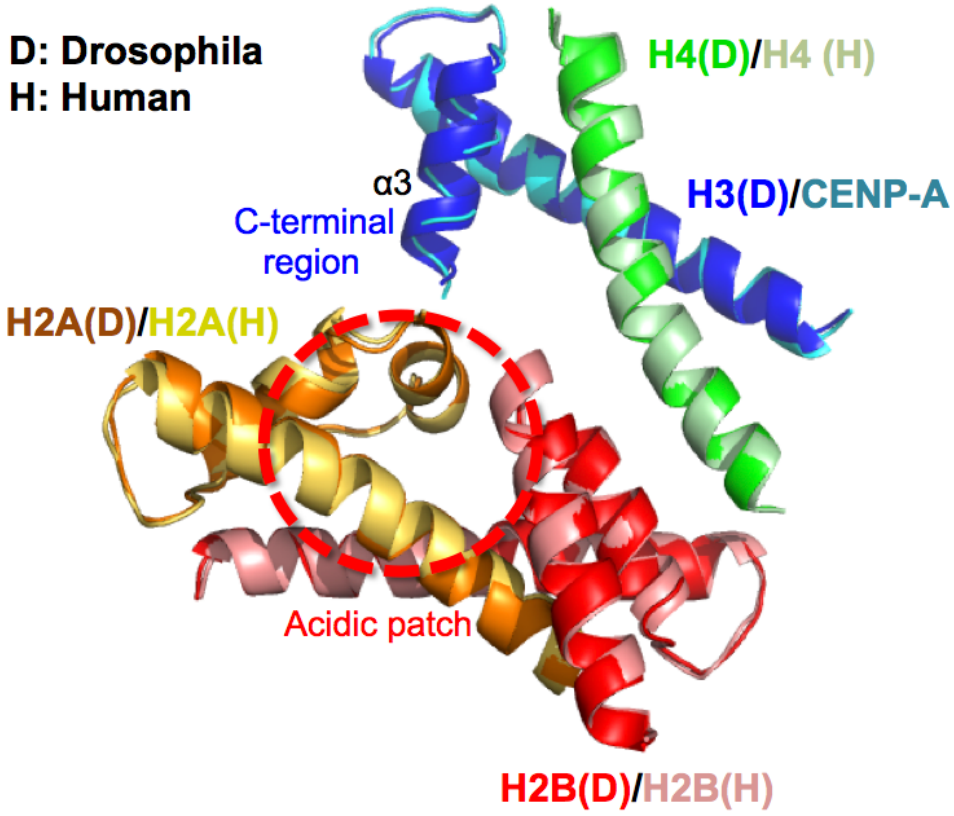

Figure S7. The binding sites of the central region of CENP-C on the $H3_{1\text{-}132}$-LEEGLG nucleosome have the same structure as the corresponding region of the human CENP-A nucleosome. Overlay of the CENP-C-binding regions in the *Drosophila* H3 nucleosome structure (pdb ID: 2PYO) with the corresponding region in the human CENP-A nucleosome (pdb ID: 3AN2). We note that the DNA entry/exit regions in the CENP-A and H3 nucleosomes, which show different dynamics, are not involved in binding of CENP-C. In addition, crystal structures of nonhistone proteins from human virus (LANA) (*17*), fly (RCC1) (*18*) and budding yeast (Sir3 BAH domain) (*19*) in complex with nucleosomes containing *Xenopus* histones have been determined successfully, showing unaltered nucleosome core structures in these complexes.

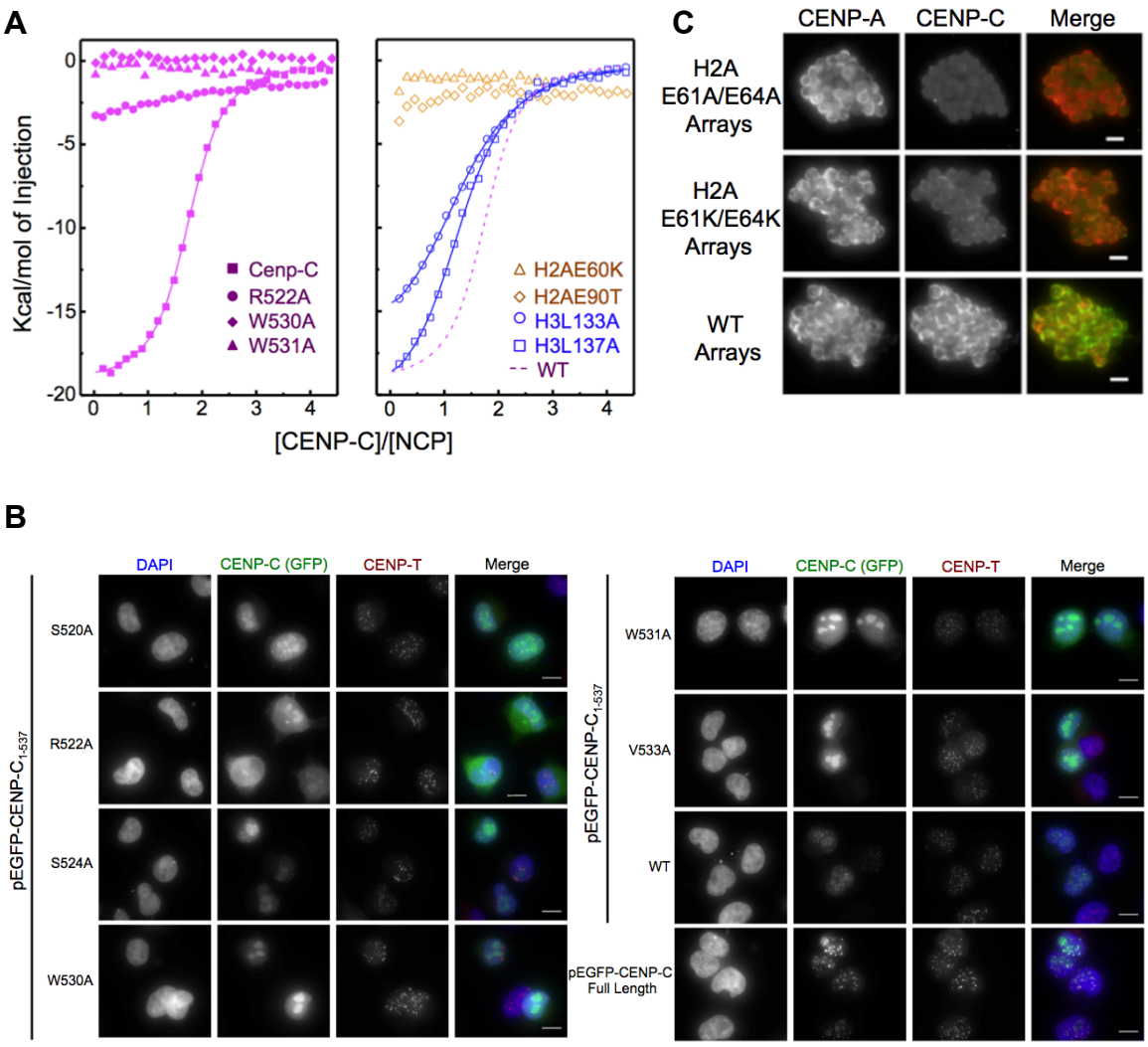

Figure S8. Residues important for binding between the central region of CENP-C and the $H3_{1-132}$-LEEGLG nucleosome. (**A**) Isothermal titration calorimetry (ITC) curves of typical mutants. (**B**) Effect of CENP-C_{1-537} mutations on centromere targeting in human cells. Fluorescence images of cells expressing GFP fusions. Scale bar = 10μm. We note that similar results also have been obtained in an earlier study (*8*). (**C**) Effect of H2A acidic patch mutations on localization of CENP-C to the CENP-A nucleosome arrays. Representative fluorescence images of chromatin arrays recovered from *Xenopus* egg extracts and immunostained for CENP-C and CENP-A. Scale bar = 5 μm. Note that Glu61 and Glu64 in human H2A corresponds to Glu60 and Glu63 in *Drosophila* H2A.

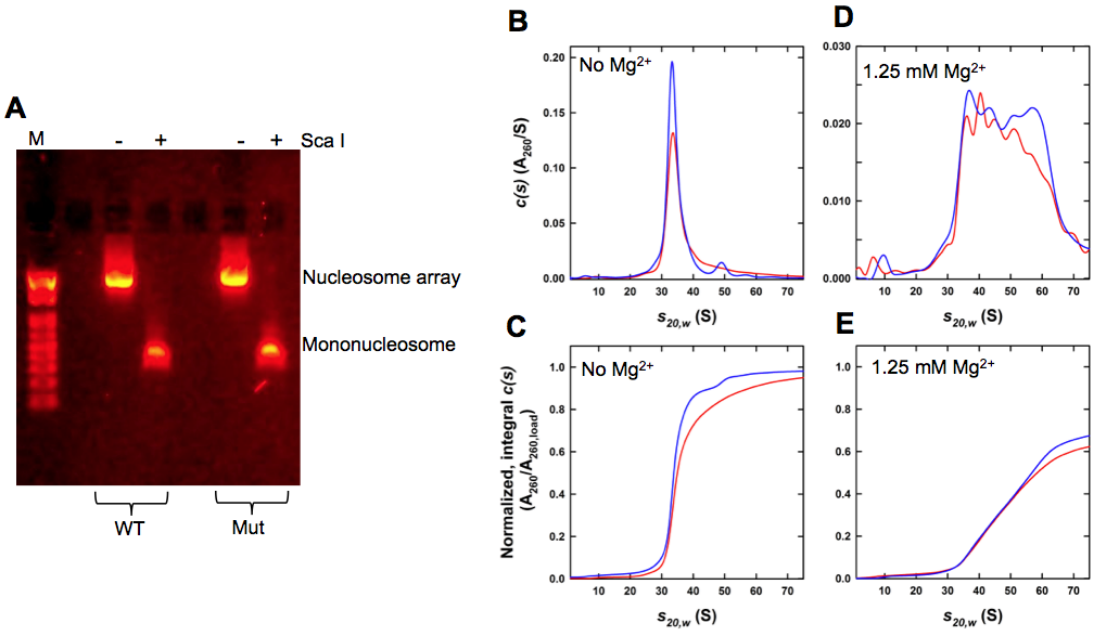

Figure S9. Neutralization of the acidic patch by the (Glu61Ala/Glu64Ala) mutation in H2A slightly increases the population of the high S value component of the nucleosome array. (**A**) Saturated CENP-A nucleosome arrays with WT histones or with H2A mutation (Glu61Ala/Glu64Ala) in the acidic patch was reconstituted using 10 x 208 bp DNA centered with "601" sequence. The middle of the linker DNA encodes a Sca I cutting site. No free DNA was found after digestion of the reconstituted arrays, indicating that the nucleosome arrays are saturated. (**B-E**) Velocity sedimentation results of the WT CENP-A nucleosome array (red) and the mutant (Glu61Ala/Glu64Ala in H2A) array (blue) (10 mM Tris-HCl, 0.25 mM EDTA, 2.5 mM NaCl, pH 7.4). These results show that the WT and mutant arrays have similar compactness, with slightly higher component at high *S* values for the mutant. In the presence of 1.25 mM Mg^{2+}, the arrays show different compact forms, consistent with the earlier observation (*39*). These results are also consistent with the observation by Luger and coworkers that neutralization of the acidic patch makes the nucleosome array easier to condense (*40*). We note that high salt concentration such as 100 mM NaCl causes aggregation of the nucleosome array. Experimental procedures and data analysis are described in an earlier publication (*41*).

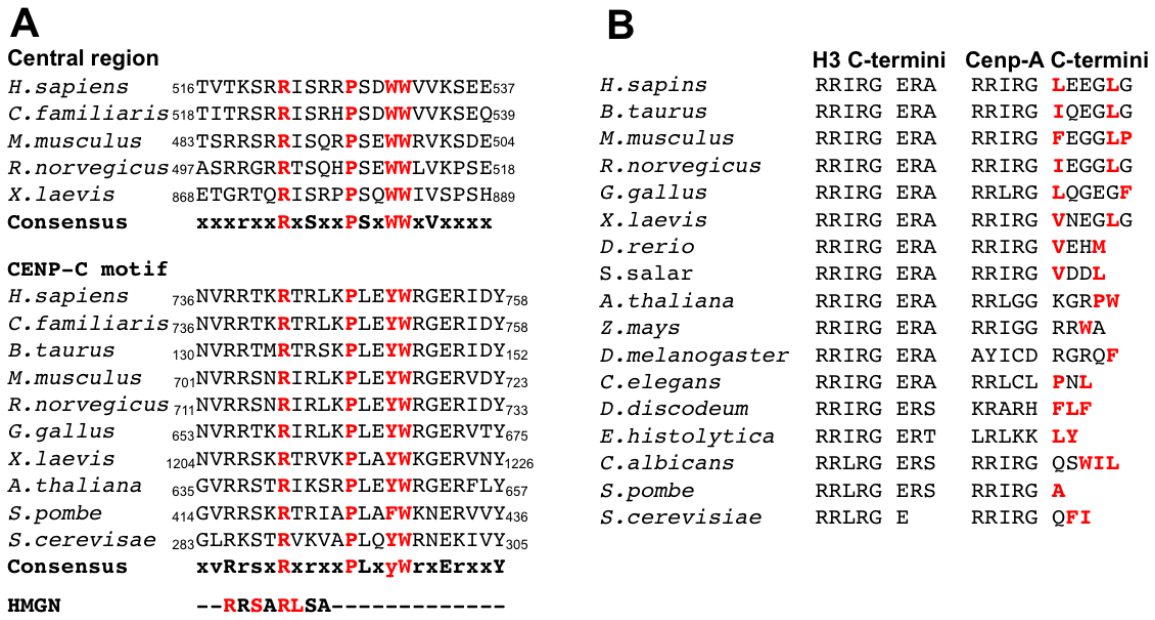

Figure S10. Conservation of critical residues between CENP-C central region and the CENP-C motif and the hydrophobic residues in the C-terminal tail of CENP-A. (**A**) Sequence comparison of the central regions of CENP-C and the CENP-C motifs from different species and the conserved HMGN region. HMGN residues important for binding of acidic patch in H2A/H2B are highlighted with bold red letters. The CENP-C motif has a consensus sequence RRS-R that also exists in the high mobility group nucleosomal (HMGN) proteins, in which the underlined residues are essential for binding of HMGNs to the acidic patch of H2A/H2B in the canonical nucleosome (*15*). (**B**) Comparison of the C-terminal tails of H3 and CENP-A in different species, showing that the C-terminal tails of CENP-A are more hydrophobic than those of corresponding H3.

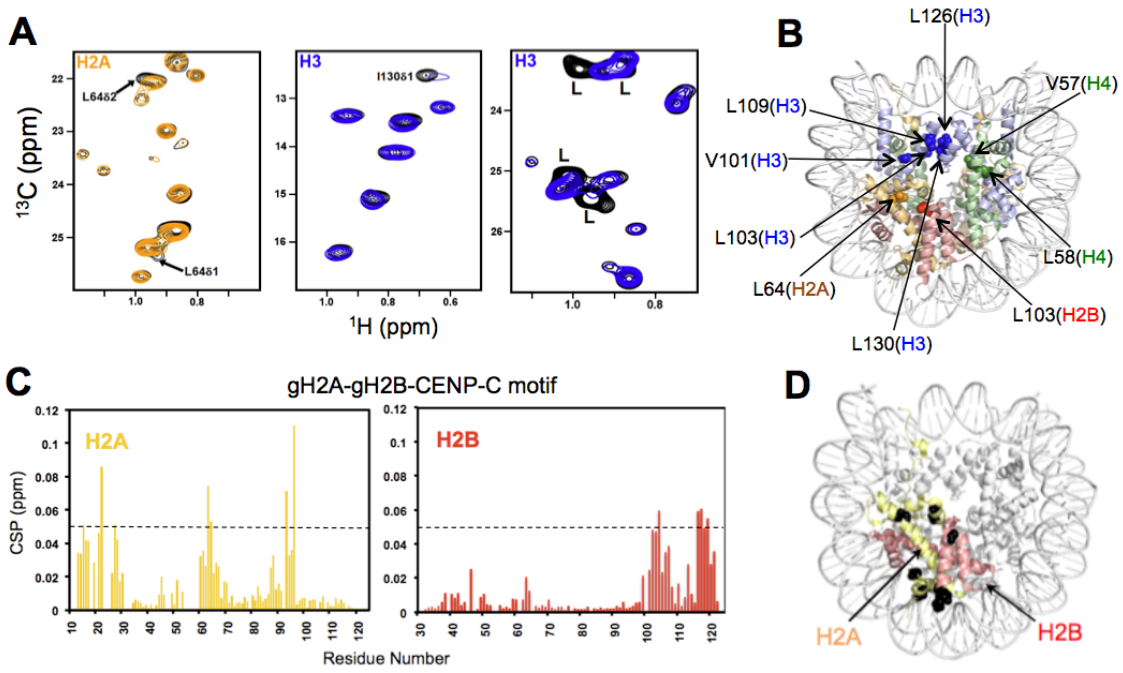

Figure S11. Chemical shift perturbation (CSP) for the interactions of the CENP-C motif with the $H3_{1-132}$-LEEGLG nucleosome and with free H2A/H2B. (**A**) Overlay of selected regions of the NMR spectra of the nucleosome containing $H3_{1-132}$-LEEGLG with (colored) and without (black) the CENP-C motif. Left: H2A; Middle: Ile residues in $H3_{1-132}$-LEEGLG; Right: Unfolded Leu residues in the LEEGLG tail of $H3_{1-132}$-LEEGLG. The strong NMR signals are from the methyl groups of the Leu residues in the LEEGLG tail of $H3_{1-132}$-LEEGLG, which disappeared upon addition of the CENP-C motif, indicating that they become folded in the complex. (**B**) Illustration of the locations of the methyl groups that show large chemical shift changes or a decrease in peak intensities. (**C**) Illustration of chemical shift changes in the free histone H2A/H2B dimer upon binding of the CENP-C motif. (**D**) Backbones of the residues with CSP larger than 0.05 in (**C**) are shown in black spheres in the H2A/H2B dimer. DNA and other histones are shown to help illustrate the binding sites on the H2A/H2B dimer.

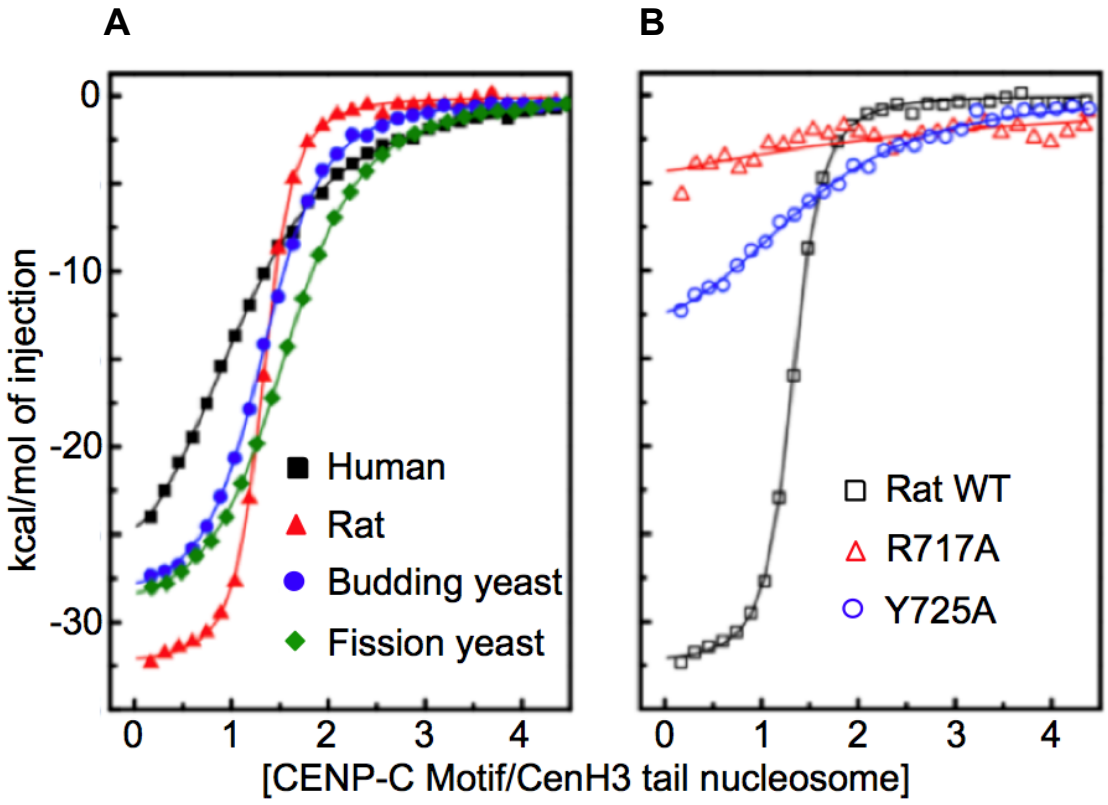

Figure S12. Broadly conserved CENP-C motifs bind to H3 nucleosome chimera containing CENP-A C-terminal tails. (**A**) ITC curves for binding of the CENP-C motifs from different species to nucleosomes containing $H3_{1-132}$ attached to the corresponding CENP-A C-terminal tails. (**B**) ITC curves for binding of rat CENP-C motif mutants to the corresponding $H3_{1-132}$-IEGGLG nucleosome. In these experiments, the nucleosome (2.5 μM) was titrated with the peptide (50 μM) corresponding to the CENP-C motif.

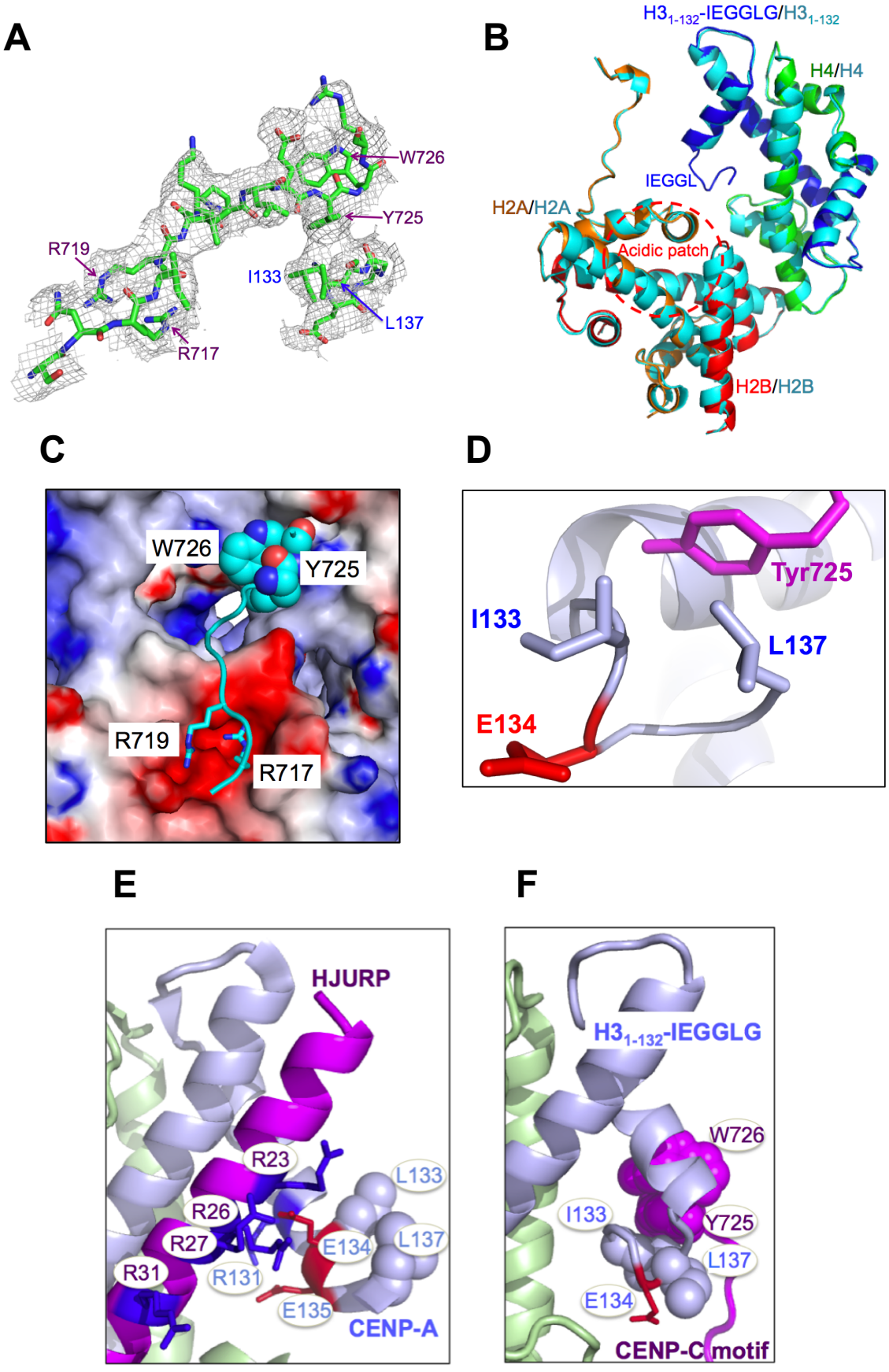
A
W726
Y725
R719
I133
L137
R717
B
H3$_{1-132}$-IEGGLG/H3$_{1-132}$
H4/H4
IEGGL
H2A/H2A
Acidic patch
H2B/H2B
C
W726
Y725
R719
R717
D
Tyr725
I133
L137
E134
E
HJURP
R23
L133
R26
R27
E134
L137
R31
R131
E135
CENP-A
F
H3$_{1-132}$-IEGGLG
W726
I133
Y725
L137
E134
CENP-C motif

Figure S13. Structural features of the rat CENP-C motif in complex with the $H3_{1-132}$-IEGGLG nucleosome complex. (**A**) Electron density maps of the CENP-C motif region and the C-terminal tail IEGGLG. Important residues are indicated. (**B**) Ribbon structures showing histone regions that are in direct contact with the CENP-C motif are not changed by CENP-C binding. Histones in complex with the CENP-C motif are shown in orange (H2A), red (H2B), blue (H3), and green (H4), respectively. Histones in the canonical nucleosome are shown in cyan. (**C**) Electrostatic potential representation (blue, positive; white, neutral; red, negative) of the binding sites of the CENP-C motif (cyan and labeled residues) (*42*). (**D**) Illustration of the turn structure formed by the IEGGLG tail. The Gly residues in the tails seem to be suitable for formation of the turn structure due to the lack of side chains. (**E**) CENP-A chaperone HJURP induces CENP-A LEEGLG tail to fold to a helical structure by forming electrostatic interactions with the two Glu residues in the tail (*43*). CENP-A tail residues L133 and L137 form intramolecule hydrophobic interactions while CENP-A residues R131 and E135 form intramolecule electrostatic interactions. (**F**) The region corresponding to (**E**) in the rat CENP-C motif in complex with the $H3_{1-132}$-IEGGLG nucleosome. The different structures of the C-terminal tail of CENP-A in (**E**) and (**F**) suggest that a conformational switch has occurred to the C-terminal tail of CENP-A after HJURP delivers the CENP-A to the centromeric nucleosome.

A

Dissociation constants for bindings of CENP-C regions to CenH3- and H3-nucleosomes.		
Human	**$H3_{1-132}$-LEEGLG**	**H3**
Central (444-537)	0.3	3.5
Motif (727-767)	1.4	5.7
Rat	**$H3_{1-132}$-IEGGLG**	**H3**
Motif (710-742)	0.1	0.8
Budding yeast	**$H3_{1-132}$-QFI**	**H3**
Motif (285-309)	0.3	3.5
	Cse4	
Motif (285-309)	0.5	3.5
Fission yeast	**$H3_{1-132}$-A**	**H3**
Motif (414-436)	1.4	16

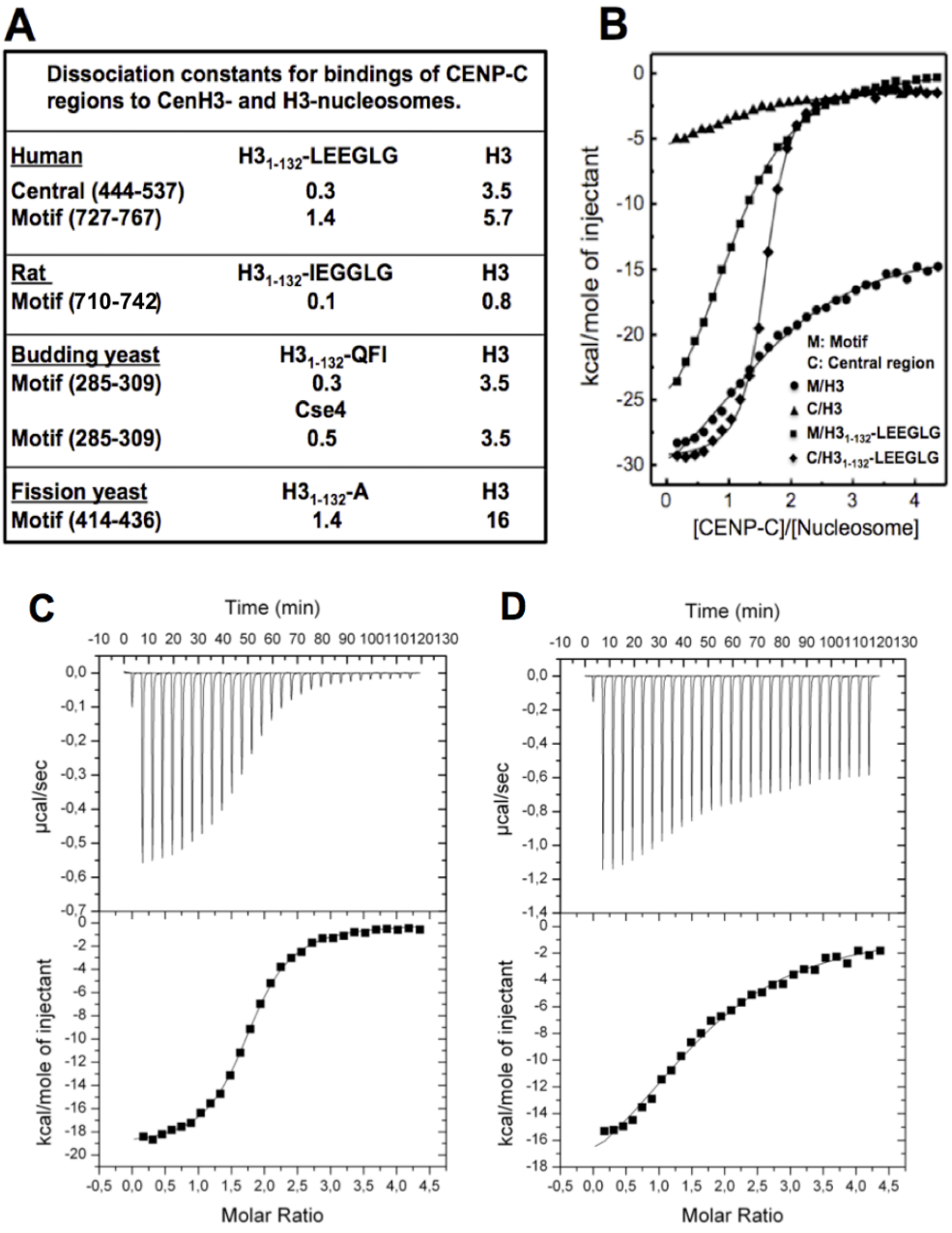

Figure S14. The central region of CENP-C and the CENP-C motif bind with higher affinities to the nucleosomes containing chimeric CENP-As than to those with H3. (**A**) Binding affinities between CENP-C regions and nucleosomes containing chimeric CENP-A and H3. The dissociation constants are in μM. (**B**) ITC results. The baselines for the titration curves are not normalized to zero. (**C, D**) ITC data for binding of the central region of CENP-C to the $H3_{1-132}$-LEEGLG and H3 nucleosomes, respectively.

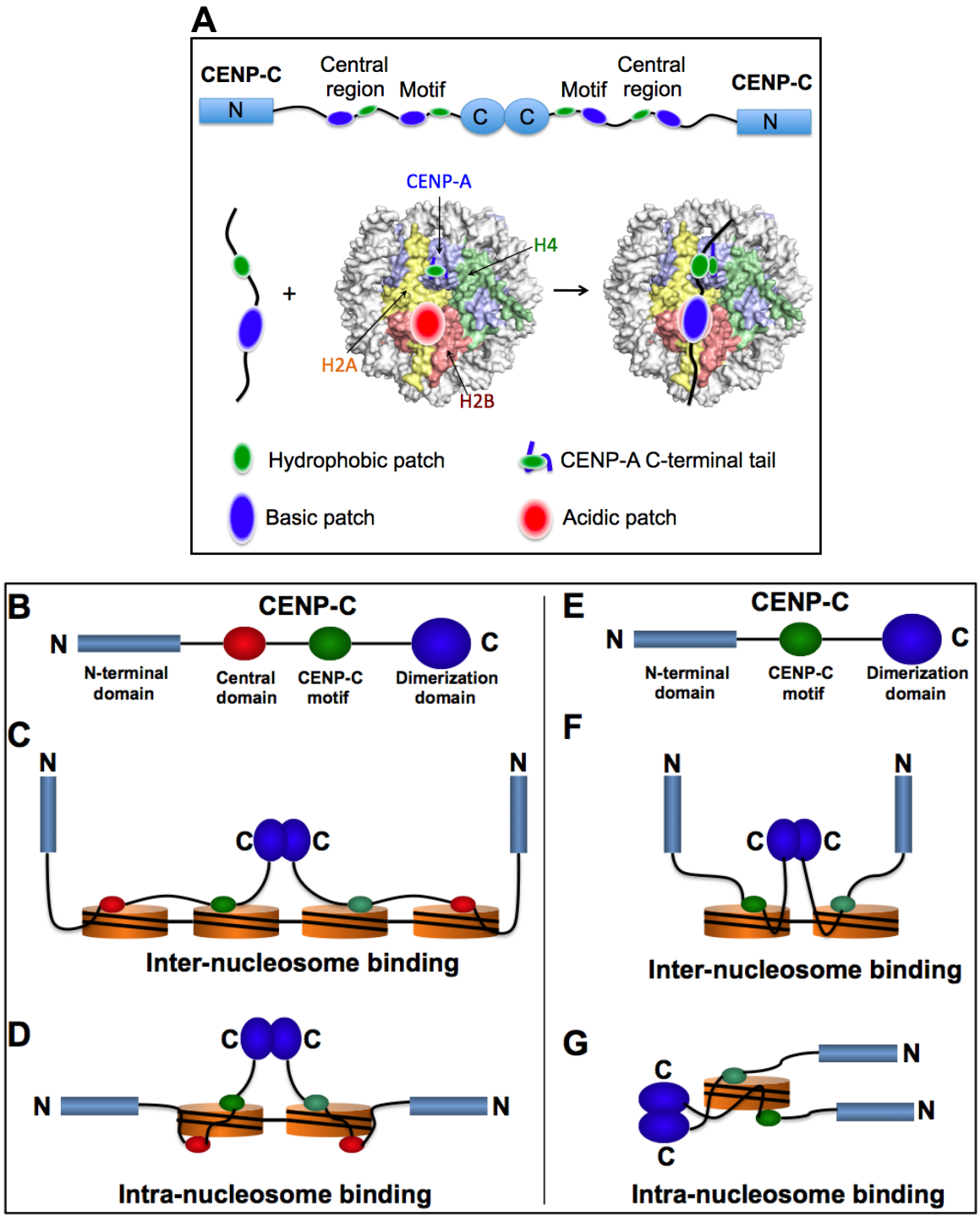

Figure S15. Models illustrating how CENP-C may bind to centromeric chromatin and enhance affinity/selectivity through multivalent interactions.

(**A**) Basic features of binding between CENP-C and the CENP-A nucleosome. (**B**) CENP-C with both the central region and the CENP-C motif. This feature of

CENP-C is consistent with the observation that full length CENP-C localizes to the centromere more efficiently than CENP-C_{1-537} (**Fig. 2B**) or CENP-$C_{584-943}$ (*20*) because the CENP-C motif in a dimeric CENP-C can also contribute to binding of the CENP-A nucleosome. (**C**) A model for inter-nucleosome binding. Orange disks represent the histone core and black lines represent DNA. (**D**) A model for intra-nucleosome binding. (**E**) CENP-C molecules that include only the CENP-C motif. (**F**) A model for inter-nucleosome binding. (**G**) A model for intra-nucleosome binding.

It should be noted that the diagrams in (**C, D, F**) are not intended to implicate specific connectivity of nucleosomes or the 3D arrangement of the nucleosomes in the centromeric chromatin; except that the nucleosomes are close in the three-dimensional space, allowing interactions with a CENP-A dimer. Available structural models of centromere chromatin generally assume that CENP-A and H3 nucleosomes form distinct clusters in the folded three-dimensional structure of the centromere chromatin while CENP-A and H3 nucleosomes may be interspersed along the one-dimensional DNA sequence (*45*).

Implications of the model:

For (**C**) and (**D**), assuming that the central region of the CENP-C and the CENP-C motif bind to the nucleosome independently, the selectivity (S) of binding of a CENP-C dimer to the CENP-A nucleosome array over that to the H3-nucleosome array may be defined as:

$$S = \{ K_d(\text{Central, H3})^2 \times K_d(\text{motif, H3})^2 \} / \{K_d(\text{Central, CENP-A})^2 \times K_d(\text{motif, CENP-A})^2\}$$

The central region of CENP-C and the CENP-C motif bind to H3-mononucleosomes ~11 and ~4 times weaker than to the corresponding nucleosomes containing $H3_{1-132}$-LEEGLG, respectively, which leads to an S value of ~2000. Therefore, the CENP-C central region and the CENP-C motif

each binds to the CENP-A nucleosome with moderate affinity, but the multivalent binding feature of the CENP-C dimer can lead to high affinity with CENP-A chromatin, which may explain why CENP-C binds to CENP-A chromatin constitutively. In addition, the central region of CENP-C alone can partially localize to the centromere (Fig. 2B) (*8*).

The moderate differences in K_d for binding of the central region of CENP-C/CENP-C motif to the CENP-A and H3 nucleosomes, along with the fact that the H3-mononucleosomes are much more abundant than the CENP-A mononucleosomes in cells, may account for the observation that CENP-C is in complex with the H3-mononucleosome when chromatin is digested with MNase to the level of mononucleosomes, whereas CENP-C is associated with the di- or tri- CENP-A nucleosomes when limited digestion of chromatin was made with MNase (*23*).

For (**G**), a single centromeric nucleosome and a dimeric Mif2 in budding yeast suggest an octameric centromeric nucleosome in association with Mif2. In this case, however, the binding of the centromeric nucleosome by the dimeric Mif2 may not be sufficient to compete with the bulk H3 nucleosomes to localize Mif2 at the centromere. Other regions of Mif2 may contribute to the selective binding of the centromeric nucleosome through alternative mechanisms. It was reported that the AT-hook of Mif2 specifically interacts with the CDEIII portion of the centromeric DNA, which could also enhance the binding specificity of Mif2 to the budding yeast centromere (*12*).

Table S1. Binding of different fragments of the central region of CENP-C to the nucleosome containing H_{1-132}-LEEGLG at pH 6.0 and 25°C.

CENP-C fragment	K_d (μM)
CENP-$C_{426-550}$	0.3
CENP-$C_{426-537}$	0.4
CENP-$C_{444-537}$	0.3
CENP-$C_{469-537}$	0.3
CENP-$C_{513-537}$	1.8
CENP-$C_{520-537}$	2.7

Table S2. Effects of mutations in the central region of CENP-C and the nucleosome containing $H3_{1-132}$-LEEGLG on their binding at pH 6 and 25 ^{o}C.

CENP-$C_{444-537}$	K_d (μM)	NCP-$H3_{1-132}$-LEEGLG	K_d (μM)
WT	0.3	WT	0.3
K519A	0.4	(E60K, H2A)	----
S520A	0.7	(E63K, H2A)	----
S520E	0.9	(D89S/E91T, H2A)	0.9
R521A	0.6	(E90T, H2A)	----
R522A	----	(E102K, H2B)	0.3
I523A	1.1	(E110K, H2B)	1.7
C472A/I523C	1.0	AEEGLG (L133A)	1.4
S524A	1.2	LAEGLG (E134A)	0.1
S524E	5.9	LEAGLG (E135A)	0.04
S520E/S524E	8.3	LEEALG (G136A)	1.0
R525A	2.6	LEEGAG (L137A)	0.9
R526A	0.6	LEEGLA (G138A)	0.5
P527A	1.8		
S528A	0.4		
D529A	0.2		
W530A	----		
W531A	----		
V532A	1.3		
V533A	2.3		

Note that Gly to Ala mutation increases K_d. Since this mutation increases the size of the side chain, it may affect the folding of the tail to a turn structure, suggesting other structural factors in addition to the hydrophobic effect may also play a role in specific recognition of CENP-C by the CENP-A tail.

Table S3. Binding of the CENP-C motif to the nucleosome at pH 7.4 and 25°C.

CENP-C motif	Nucleosome	K_d (μM)
Human		
CENP-$C_{727-767}$	$H3_{1-132}$-LEEGLG	1.4
CENP-$C_{727-767}$	$H3_{1-132}$(CATD)-LEEGLG*	1.3
CENP-$C_{735-767}$	$H3_{1-132}$-LEEGLG	2.6
CENP-$C_{727-767}$	$H3_{1-132}$-LEEGLG (H2A E60K)	----
CENP-$C_{727-767}$	$H3_{1-132}$-LEEGLG (H2A E63K)	----
CENP-$C_{727-767}$	$H3_{1-132}$-QFI	3.0
CENP-$C_{444-537}$	$H3_{1-132}$-QFI	0.2
Rat		
CENP-$C_{710-742}$	$H3_{1-132}$-IEGGLG	0.1
Fission yeast		
CENP-$C_{414-436}$	$H3_{1-132}$-A	1.4
Budding yeast		
$Mif2_{285-309}$	$H3_{1-132}$-QFI	0.3
$Mif2_{285-309}$	Cse4	0.5

* The L1 loop and α2 helix of H3 were substituted with the corresponding region (CATD: CENP-A targeting domain) of CENP-A (*44*), which involves 22 mutations. The unchanged binding affinity further supports the use of $H3_{1-132}$-LEEGLG to substitute for CENP-A for structural study.

Table S4. Mutation effects on the binding of the rat CENP-C motif (CENP-$C_{710-742}$) to the nucleosome containing $H3_{1-132}$-IEGGLG at pH 7.4 and 25^{o}C.

CENP-C motif	K_d (μM)
WT	0.1
R713A	0.6
R714A	0.2
S715A	0.5
R717A	----
R719A	0.3
P722A	0.1
L723A	0.1
Y725A	1.1
Y725F	0.1
W726A	0.4
W726R	0.9
R727A	0.5
E729K	0.3
Y733A	0.03

Table S5. X-ray diffraction data collection and structural refinement statistics.

Data Collection	
Space group	$P2_12_12_1$
Unit cell (a, b, c) (Å)	103.0, 176.1, 208.9
(α, β, γ) (°)	90.0, 90.0, 90.0
Wavelength (Å)	1.033
Resolution (Å)	50-3.50 (3.55-3.50)*
No. of reflections (total/unique)	200687/46684
Redundancy	4.0 (3.0) *
Completeness (%)	96.1 (78.7)*
I/σ(I)	11.0 (1.5)*
R_{merge} (%)¶	11.8 (69.5)*
R_{pim} (%)§	6.4 (49.1) *
Refinement	
Resolution (Å)	50-3.50 (3.55-3.50)
Number of atoms	24004
Histones	11470
DNA	12070
CENP-C	464
B-factor (Å^2)	176.8
Histones	118.9
DNA	205.4
CENP-C	140.8
Rmsd bond lengths (Å)	0.006
Rmsd bond angles (°)	1.082
R_{work} (%)†	23.5 (37.9) *
R_{free} (%)‡	28.7 (39.5) *
Ramachandran plot favored/disallowed**	90.6/0.8

PDB code	4INM

*Asterisked numbers correspond to the last resolution shell.

¶ R_{merge} = $\Sigma_h \Sigma_i |I_i(h) - \langle I(h) \rangle| / \Sigma_h \Sigma_i I_i(h)$, where $I_i(h)$ and $\langle I(h) \rangle$ are the ith and mean measurement of the intensity of reflection *h*.

§ $R_{pim} = \Sigma h [(1/n-1)^{1/2}] \Sigma i |Ii(h) - \langle I(h) \rangle| / \Sigma h \Sigma i Ii(h)$, where Ii(*h*) and $\langle I(h) \rangle$ are the ith and mean measurement of the intensity of reflection *h*, and n is the redundancy of reflection *h*.

† $R_{work} = \Sigma_h ||F_{obs}(h)| - |F_{calc}(h)|| / \Sigma_h |F_{obs}(h)|$, where $F_{obs}(h)$ and $F_{calc}(h)$ are the observed and calculated structure factors, respectively.

‡ R_{free} is the R value obtained for a test set of reflections consisting of a randomly selected 5% subset of the dataset excluded from refinement.

**Values from Molprobity server (http://molprobity.biochem.duke.edu/).

References

1. S. Henikoff, K. Ahmad, H. S. Malik, The centromere paradox: Stable inheritance with rapidly evolving DNA. *Science* **293**, 1098 (2001). doi:10.1126/science.1062939 Medline

2. J. S. Verdaasdonk, K. Bloom, Centromeres: Unique chromatin structures that drive chromosome segregation. *Nat. Rev. Mol. Cell Biol.* **12**, 320 (2011). doi:10.1038/nrm3107 Medline

3. T. Hori *et al*., CCAN makes multiple contacts with centromeric DNA to provide distinct pathways to the outer kinetochore. *Cell* **135**, 1039 (2008). doi:10.1016/j.cell.2008.10.019 Medline

4. M. R. Przewloka *et al*., CENP-C is a structural platform for kinetochore assembly. *Curr. Biol.* **21**, 399 (2011). doi:10.1016/j.cub.2011.02.005 Medline

5. C. W. Carroll, K. J. Milks, A. F. Straight, Dual recognition of CENP-A nucleosomes is required for centromere assembly. *J. Cell Biol.* **189**, 1143 (2010). doi:10.1083/jcb.201001013 Medline

6. A. Guse, C. W. Carroll, B. Moree, C. J. Fuller, A. F. Straight, In vitro centromere and kinetochore assembly on defined chromatin templates. *Nature* **477**, 354 (2011). doi:10.1038/nature10379 Medline

7. E. Screpanti *et al*., Direct binding of Cenp-C to the Mis12 complex joins the inner and outer kinetochore. *Curr. Biol.* **21**, 391 (2011). doi:10.1016/j.cub.2010.12.039 Medline

8. K. Song, B. Gronemeyer, W. Lu, E. Eugster, J. E. Tomkiel, Mutational analysis of the central centromere targeting domain of human centromere protein C (CENP-C). *Exp. Cell Res.* **275**, 81 (2002). doi:10.1006/excr.2002.5495 Medline

9. K. J. Milks, B. Moree, A. F. Straight, Dissection of CENP-C-directed centromere and kinetochore assembly. *Mol. Biol. Cell* **20**, 4246 (2009). doi:10.1091/mbc.E09-05-0378 Medline

10. K. Tanaka, H. L. Chang, A. Kagami, Y. Watanabe, CENP-C functions as a scaffold for effectors with essential kinetochore functions in mitosis and meiosis. *Dev. Cell* **17**, 334 (2009). doi:10.1016/j.devcel.2009.08.004 Medline

11. S. Heeger *et al*., Genetic interactions of separase regulatory subunits reveal the diverged *Drosophila* Cenp-C homolog. *Genes Dev.* **19**, 2041 (2005). doi:10.1101/gad.347805 Medline

12. R. L. Cohen *et al*., Structural and functional dissection of Mif2p, a conserved DNA-binding kinetochore protein. *Mol. Biol. Cell* **19**, 4480 (2008). doi:10.1091/mbc.E08-03-0297 Medline

13. C. W. Carroll, M. C. Silva, K. M. Godek, L. E. Jansen, A. F. Straight, Centromere assembly requires the direct recognition of CENP-A nucleosomes by CENP-N. *Nat. Cell Biol.* **11**, 896 (2009). doi:10.1038/ncb1899 Medline

14. V. Tugarinov, V. Kanelis, L. E. Kay, Isotope labeling strategies for the study of high-molecular-weight proteins by solution NMR spectroscopy. *Nat. Protoc.* **1**, 749 (2006). doi:10.1038/nprot.2006.101 Medline

15. H. Kato *et al*., Architecture of the high mobility group nucleosomal protein 2-nucleosome complex as revealed by methyl-based NMR. *Proc. Natl. Acad. Sci. U.S.A.* **108**, 12283 (2011). doi:10.1073/pnas.1105848108 Medline

16. H. Tachiwana *et al*., Crystal structure of the human centromeric nucleosome containing CENP-A. *Nature* **476**, 232 (2011). doi:10.1038/nature10258 Medline

17. A. J. Barbera *et al*., The nucleosomal surface as a docking station for Kaposi's sarcoma herpesvirus LANA. *Science* **311**, 856 (2006). doi:10.1126/science.1120541 Medline

18. R. D. Makde, J. R. England, H. P. Yennawar, S. Tan, Structure of RCC1 chromatin factor bound to the nucleosome core particle. *Nature* **467**, 562 (2010). doi:10.1038/nature09321 Medline

19. K. J. Armache, J. D. Garlick, D. Canzio, G. J. Narlikar, R. E. Kingston, Structural basis of silencing: Sir3 BAH domain in complex with a nucleosome at 3.0 Å resolution. *Science* **334**, 977 (2011). doi:10.1126/science.1210915 Medline

20. S. Trazzi *et al*., In vivo functional dissection of human inner kinetochore protein CENP-C. *J. Struct. Biol.* **140**, 39 (2002).

21. A. Philpott, G. H. Leno, Nucleoplasmin remodels sperm chromatin in *Xenopus* egg extracts. *Cell* **69**, 759 (1992). doi:10.1016/0092-8674(92)90288-N Medline

22. G. Wieland, S. Orthaus, S. Ohndorf, S. Diekmann, P. Hemmerich, Functional complementation of human centromere protein A (CENP-A) by Cse4p from *Saccharomyces cerevisiae*. *Mol. Cell. Biol.* **24**, 6620 (2004). doi:10.1128/MCB.24.15.6620-6630.2004 Medline

23. S. Ando, H. Yang, N. Nozaki, T. Okazaki, K. Yoda, CENP-A, -B, and -C chromatin complex that contains the I-type alpha-satellite array constitutes the prekinetochore in HeLa cells. *Mol. Cell. Biol.* **22**, 2229 (2002). doi:10.1128/MCB.22.7.2229-2241.2002 Medline

24. B. E. Black, D. W. Cleveland, Epigenetic centromere propagation and the nature of CENP-a nucleosomes. *Cell* **144**, 471 (2011). doi:10.1016/j.cell.2011.02.002 Medline

25. L. J. Bock *et al*., Cnn1 inhibits the interactions between the KMN complexes of the yeast kinetochore. *Nat. Cell Biol.* **14**, 614 (2012). doi:10.1038/ncb2495 Medline

26. A. Schleiffer *et al*., CENP-T proteins are conserved centromere receptors of the Ndc80 complex. *Nat. Cell Biol.* **14**, 604 (2012). doi:10.1038/ncb2493 Medline

27. S. Khorasanizadeh, Recognition of methylated histones: New twists and variations. *Curr. Opin. Struct. Biol.* **21**, 744 (2011). doi:10.1016/j.sbi.2011.10.001 Medline

28. C. A. Musselman, M. E. Lalonde, J. Côté, T. G. Kutateladze, Perceiving the epigenetic landscape through histone readers. *Nat. Struct. Mol. Biol.* **19**, 1218 (2012). doi:10.1038/nsmb.2436 Medline

29. F. Delaglio *et al*., NMRPipe: A multidimensional spectral processing system based on UNIX pipes. *J. Biomol. NMR* **6**, 277 (1995). doi:10.1007/BF00197809 Medline

30. Z. Otwinowski, W. Minor, Processing of x-ray diffraction data collected in oscillation mode. *Methods Enzymol.* **276**, 307 (1997).

31. W. Kabsch, XDS. *Acta Crystallogr. D* **66**, 125 (2010). doi:10.1107/S0907444909047337 Medline

32. C. R. Clapier *et al*., Structure of the *Drosophila* nucleosome core particle highlights evolutionary constraints on the H2A-H2B histone dimer. *Proteins* **71**, 1 (2008). doi:10.1002/prot.21720 Medline

33. A. J. McCoy *et al*., *Phaser* crystallographic software. *J. Appl. Crystallogr.* **40**, 658 (2007). doi:10.1107/S0021889807021206

34. P. D. Adams *et al*., PHENIX: A comprehensive Python-based system for macromolecular structure solution. *Acta Crystallogr. D* **66**, 213 (2010). doi:10.1107/S0907444909052925 Medline

35. A. T. Brünger *et al*., Application of DEN refinement and automated model building to a difficult case of molecular-replacement phasing: The structure of a putative succinyl-diaminopimelate desuccinylase from *Corynebacterium glutamicum*. *Acta Crystallogr. D* **68**, 391 (2012). doi:10.1107/S090744491104978X Medline

36. A. T. Brünger *et al*., Crystallography & NMR system: A new software suite for macromolecular structure determination. *Acta Crystallogr. D* **54**, 905 (1998). doi:10.1107/S0907444998003254 Medline

37. V. B. Chen *et al*., MolProbity: All-atom structure validation for macromolecular crystallography. *Acta Crystallogr. D* **66**, 12 (2010). doi:10.1107/S0907444909042073 Medline

38. C. Dominguez, R. Boelens, A. M. J. J. Bonvin, HADDOCK: A protein-protein docking approach based on biochemical or biophysical information. *J. Am. Chem. Soc.* **125**, 1731 (2003). doi:10.1021/ja026939x Medline

39. T. Panchenko *et al*., Replacement of histone H3 with CENP-A directs global nucleosome array condensation and loosening of nucleosome superhelical termini. *Proc. Natl. Acad. Sci. U.S.A.* **108**, 16588 (2011). doi:10.1073/pnas.1113621108 Medline

40. J. V. Chodaparambil *et al*., A charged and contoured surface on the nucleosome regulates chromatin compaction. *Nat. Struct. Mol. Biol.* **14**, 1105 (2007). doi:10.1038/nsmb1334 Medline

41. B.-R. Zhou *et al*., Histone H4 K16Q mutation, an acetylation mimic, causes structural disorder of its N-terminal basic patch in the nucleosome. *J. Mol. Biol.* **421**, 30 (2012). doi:10.1016/j.jmb.2012.04.032 Medline

42. B. Honig, A. Nicholls, Classical electrostatics in biology and chemistry. *Science* **268**, 1144 (1995). doi:10.1126/science.7761829 Medline

43. H. Hu *et al*., Structure of a CENP-A-histone H4 heterodimer in complex with chaperone HJURP. *Genes Dev.* **25**, 901 (2011). doi:10.1101/gad.2045111 Medline

44. B. E. Black *et al*., Structural determinants for generating centromeric chromatin. *Nature* **430**, 578 (2004). doi:10.1038/nature02766 Medline

45. R. C. Allshire, G. H. Karpen, Epigenetic regulation of centromeric chromatin: Old dogs, new tricks? *Nat. Rev. Genet.* **9**, 923 (2008). doi:10.1038/nrg2466 Medline